Multimutated Herpes Simplex Virus G207 Is a Potent Inhibitor of Angiogenesis[1]

*Jindrich Cinatl Jr.**, Martin Michaelis**,[2], Pablo Hernáiz Driever*[†,2], Jaroslav Cinatl**, Jan Hrabeta*[‡], Tatyana Suhan**, Hans Wilhelm Doerr** and Jens-Uwe Vogel**

*Institute of Medical Virology, Center of Hygiene, Paul-Ehrlich Str. 40, Frankfurt am Main D-60596, Germany; [†]Department of Pediatric Oncology and Hematology, Charité Medical Center, Campus Virchow Hospital, Humboldt University, Augustenburger Platz 1, Berlin D-13353, Germany; [‡]Department of Pediatric Hematology and Oncology, 2nd Faculty of Medicine, Charles University, V Úvalu 84, Praha 5, 150 06, Czech Republic

Abstract

The mode of the antitumoral activity of multimutated oncolytic herpes simplex virus type 1 G207 has not been fully elucidated yet. Because the antitumoral activity of many drugs involves the inhibition of tumor blood vessel formation, we determined if G207 had an influence on angiogenesis. Monolayers of human umbilical vein endothelial cells and human dermal microvascular endothelial cells, but not human dermal fibroblasts, bronchial epithelial cells, and retinal glial cells, were highly sensitive to the replicative and cytotoxic effects of G207. Moreover, G207 infection caused the destruction of endothelial cell tubes *in vitro*. In the *in vivo* Matrigel plug assay in mice, G207 suppressed the formation of perfused vessels. Intratumoral treatment of established human rhabdomyosarcoma xenografts with G207 led to the destruction of tumor vessels and tumor regression. Ultrastructural investigations revealed the presence of viral particles in both tumor and endothelial cells of G207-treated xenografts, but not in adjacent normal tissues. These findings show that G207 may suppress tumor growth, in part, due to inhibition of angiogenesis.

Neoplasia (2004) **6**, 725–735

Keywords: Angiogenesis, HSV-1, G207, human rhabdomyosarcoma, ribonucleotide reductase.

Introduction

Viruses used for oncolytic therapy replicate selectively in transformed cells, killing them through a direct cytopathic effect and enabling the viral progeny to spread within the tumor, sparing nontransformed surrounding cells [1]. Herpes simplex virus type 1 (HSV-1) G207 was initially designed for clinical use in malignant brain tumor patients. Experimental studies demonstrated its efficiency also against human carcinoma cell lines of the breast [2], prostate [3], colon [4], ovaries [5], head and neck squamous cells [6], malignant melanoma [7], as well as pediatric solid tumors such as neuroblastoma [8,9], rhabdomyosarcoma [10,11], and osteosarcoma [10]. G207 harbors deletions in both copies of the γ*34.5* gene, the major determinant of HSV-1 neurovirulence [12,13], and carries an insertion of the *Escherichia coli lacZ* gene in the viral *ICP6* gene (UL39), inactivating viral ribonucleotide reductase (RR) [14]. Because viral replication can only take place in the presence of RR, replication of G207 is limited to dividing cells expressing high levels of cellular RR [15,16]. Insertion of a *lacZ* marker gene, which produces a histochemically identifiable protein product, enables easy detection of virus-infected cells [17]. The multiple mutations of HSV-1 G207 minimize the chance of reversion to wild-type virus and confer additional safety features such as sensitivity to ganciclovir and temperature sensitivity, which halts viral activity in the febrile host [17,18].

In the past decades, increased interest has been focusing on the role of new blood vessel formation in the pathogenesis of tumors [19,20]. In addition to specific antiangiogenic agents, virtually every conventional cytotoxic anticancer drug has been ''accidentally'' discovered to have antiangiogenic effects in various *in vivo* models [21,22]. In the present study, we tested the sensitivity of endothelial cells to G207 and the ability of the virus to inhibit angiogenesis *in vitro* and *in vivo*.

Materials and Methods

Virus

G207 was kindly provided by NeuroVir (Vancouver, Canada). The wild type of HSV-1 (strain McIntyre) was purchased from ATCC (Manassas, VA). Viral stocks were prepared by infecting African green monkey kidney cells (Vero;

Abbreviations: HSV-1, herpes simplex virus type 1; HUVEC, human umbilical vein endothelial cells; HDMEC, human dermal microvascular endothelial cells; HRG, retinal glial cells; NHBE, normal human bronchial epithelial cells; RR, ribonucleotide reductase; IMDM, Iscove's modified Dulbecco's medium; bFGF, basic fibroblast growth factor; MEM, minimal essential medium; MOI, multiplicity of infection; X-gal, 5-bromo-4-chloro-3-indolyl-β-D-galactopyranoside; PFU, plaque-forming units

Address all correspondence to: Jindrich Cinatl, Jr., PhD, Institute of Medical Virology, Center of Hygiene, Paul-Ehrlich Str., 40, Frankfurt am Main D-60596, Germany. E-mail: Cinatl@em.uni-frankfurt.de

[1]This work was generously supported by the friendly society ''Hilfe für krebskranke Kinder Frankfurt eV'' and its foundation ''Frankfurter Stiftung für krebskranke Kinder.''

[2]Martin Michaelis and Pablo Hernáiz Driever equally contributed to this paper.

Received 2 April 2004; Revised 10 June 2004; Accepted 18 June 2004.

DOI 10.1593/neo.04265

ATCC) cultured in MEM supplemented with 5% inactivated fetal calf serum (FCS) at a multiplicity of infection (MOI) of 0.01 at 34°C and by harvesting the virus when a complete cytopathic effect was observed. After a freeze–thaw/sonication regime, cell debris was removed by low-speed centrifugation (2000*g* for 10 minutes at 4°C). G207 was concentrated by subsequent high-speed centrifugation (45,000*g* for 150 minutes at 4°C). The viral pellet was then resuspended in 150 mM NaCl and 20 mM Tris, pH 7.5. Infectious titers of viral stocks were determined by plaque titration on Vero cell monolayers as described previously [11] and stored at −80°C before use.

To investigate whether antiangiogenic effects of G207 were attributed to viral replication, inactivated G207 was used as a control. Inactivation of the virus was achieved by the exposure of viral solution to UVB light (280–350 nm, peak at 306 nm) for 25 minutes, delivering approximately 3.6 J/cm^2. UV-irradiated virus suspensions were free of infectious virus as demonstrated by plaque titration using Vero cell monolayers.

Cells

Human umbilical vein endothelial cells (HUVEC) were isolated and cultured in Iscove's modified Dulbecco's medium (IMDM; Sigma, Taufkirchen, Germany) supplemented with 10% FCS, 10% pooled human serum (Blood Bank of the German Red Cross, Frankfurt am Main, Germany), 100 IU/ml penicillin, 100 μg/ml streptomycin, and 5 ng/ml basic fibroblast growth factor (bFGF), as described previously [23]. Human dermal microvascular endothelial cells (HDMEC) were obtained from PromoCell (Heidelberg, Germany). Cells were cultured according to the instructions of the producer using endothelial cell growth medium MV (PromoCell). Normal human bronchial epithelial cells (NHBE) were obtained from Clonetics (CellSystems, St. Katharinen, Germany) and cultured in BEGM medium according to the instructions of the producer. Human foreskin fibroblasts (HFF) and retinal glial cells (HRG) were isolated and cultivated as described previously using IMDM supplemented with 10% FBS, 100 IU/ml penicillin, and 100 μg/ml streptomycin [24]. The human alveolar rhabdomyosarcoma (ARMS) cell line, KFR, was established in our laboratory from bone marrow metastases of a patient suffering from ARMS [25]. KFR cells were grown in IMDM supplemented with 10% FCS, 100 IU/ml penicillin, and 100 μg/ml streptomycin. Cells were routinely tested for *Mycoplasma* and found to be free of contamination.

Oncolysis of Human Cultured Cells

For *in vitro* susceptibility assays, cultured cells were plated in six-well dishes at a density of 5×10^4 cells/cm^2. After 72 hours, confluent cell layers were infected with G207 at an MOI of 0.1, or mock-infected with viral buffer alone. After an adsorption period (90 minutes) at 37°C, infected cells were maintained in growth medium containing 1% heat-inactivated FCS at 37°C. Viable cells were counted in a hemocytometer using the trypan blue exclusion method at different times postinfection.

In some experiments, endothelial cells were treated with inhibitors of RR including DFO (6.25–100 μM concentrations) and hydroxyurea (125–1000 μM), or inhibitors of Ras/Raf/MEK/Erk cascade including farnesyltransferase inhibitor manumycin A (5–40 μM) and MEK inhibitor PD98059 (5–40 μM). The inhibitors were added 2 hours before infection.

Immunoblotting

Cells were lysed in sodium dodecyl sulfate (SDS) sample buffer and separated by SDS-PAGE, as described previously [23]. In brief, proteins were detected using specific antibodies against Erk1/2 and its phoshorylated form, phosphoro-Erk1/2 (Cell Signaling, Beverly, MA), actin (Sigma), or M1 subunit of human RR (Biomol, Hamburg, Germany), and were visualized by enhanced chemiluminescence using a commercially available kit (Amersham, Braunschweig, Germany).

Infection Efficiency and Viral Growth of HSV-1 G207 in Cultured Cells

To evaluate the infection efficiency of G207 in different cell cultures, X-gal (Sigma) staining was performed using a previously described technique [11]. The percentage of *lacZ*-positive cells was calculated as a measure of infection 3 days after infection. To assess the replication capacity of virus, viral titers were measured in different cell types. Cells were incubated with G207 at an MOI of 0.1 for an adsorption period (90 minutes) and washed three times with PBS, and maintenance medium was added. Immediately after virus adsorption (input virus titer) or different times postinfection, cultures were subjected to three cycles of freeze–thaw lysis, sonication, and centrifugation at 2000*g* for 10 minutes at 4°C. Infectious titers of supernatants were determined on confluent Vero cell layers, as described above.

In Vitro Matrigel Angiogenesis Assay

The assay was performed as described previously [23]. Briefly, 96-well plates were coated with cold Matrigel (50 μl/well), which was allowed to polymerize at room temperature for about 30 minutes. HUVEC were mock-infected, infected with G207, or infected with UVB-inactivated G207. After 1 hour of adsorption and infection, cells were washed and 100 μl of a suspension of differently treated HUVEC (5×10^4 cells/ml) was seeded onto Matrigel in IMDM, supplemented with 100 IU/ml penicillin, 100 μg/ml streptomycin, 1% (vol/vol) FCS, and 5 ng/ml bFGF. In some experiments, acyclovir at a concentration of 20 μM was added to cultures of G207-infected cells. Tube formation was assessed after 48 hours and quantified by counting of branching points.

In Vivo Matrigel Plug Assay

All animal experiments were performed according to the guidelines for the use of vertebrate animals of the Charles University (Prague, Czech Republic). C57/BL6 mice (AnLab Ltd., Prague, Czech Republic) were used for Matrigel plug assay. Matrigel (0.5 ml) supplemented with 75 ng bFGF was injected subcutaneously into the flank. Solvent (saline), G207, or UVB-inactivated G207 (all in a volume of 50 μl) was

injected into the plug on days 1 and 3 after Matrigel injection. On day 10, animals were sacrificed, and the Matrigel plug together with surrounding tissue were removed. The tissue was fixed overnight in phosphate-buffered saline containing 10% formalin and 0.25% glutaraldehyde, embedded into paraffin, and stained with Masson's trichrome, as described previously [23]. This procedure stains the Matrigel blue and endothelial cells/vessels red. To quantify the extent of angiogenesis, perfused blood vessels were counted.

Subcutaneous Xenotransplanted Tumor Model of Human Rhabdomyosarcoma

Female outbred athymic nude mice, strain CD-1 (nu/nu), about 20 g of weight (AnLab Ltd., Charles River, Czech Republic), were used for experiments. Mice were kept under sterile conditions, receiving sterile nutrition and water. A total of 1×10^7 human KFR cells were injected subcutaneously together with Matrigel in a total volume of 0.2 ml into the right flank of mice. Tumor volumes were determined using a caliper and calculated by the formula: Volume = (length $\times$ width^2)/2. The longer side was defined to be the length and the shorter one was defined to be the width.

Intraneoplastic Treatment of Human Rhabdomyosarcoma Tumors with HSV-1 G207

Xenotransplanted KFR tumors were established as described above. After tumor cell inoculation, mice were randomly divided into groups of seven animals. When tumors reached a size of about 100 mm^3, treatment was started. This day was defined to be day 0. Animals received 1×10^7 plaque-forming units (PFU) G207 intratumorally, suspended in a volume of 20 μl of virus buffer on days 0 and 4. Control animals received intratumoral virus buffer or UVB-inactivated G207 virus suspension.

Immunohistochemical Analysis

To detect endothelial cells in tumor tissues, immunohistochemical analysis of subcutaneous KFR tumors treated with saline (control) or G207-treated tumors was performed. Tumors excised from sacrificed animals were rinsed with sterile PBS, fixed in 10% neutral-buffered formalin, embedded into paraffin, and sectioned. Thin sections were examined with immunoperoxidase, carried out using a rabbit anti–mouse Factor VIII antiserum (DakoCytomation, Hamburg, Germany). Slides were then subjected to avidin–biotin–horseradish peroxidase staining and counterstained in hematoxylin. The numbers of Factor VIII–stained vessels were counted by two independent observers in tumor tissue areas, which included higher vessel density (hot spot).

Reverse Transcription Polymerase Chain Reaction (RT-PCR)

Total RNA was isolated from HUVEC (mock- and G207-infected, with or without DFO treatment) using TRIZOL according to the manufacturer's instructions (Gibco-BRL Life Technologies, Gaithersburg, MD). RNA was reverse-transcribed using random hexamer priming, as described previously [26]. mRNA levels of the viral genes α (α27), β (UL30), and γ (UL44) were detected using the following primers [27]: for α27, 5′-CTGGAATCGGACAGCAGCCGG-3′ and 5′-GAGGCGCGACCACACACTGT-3′, which yield a 222-bp fragment; for UL30, 5′-ATCAACTTCGACTGGCCCTTC-3′ and 5′-CCGTACATGTCGATGTTCACC-3′, producing a 180-bp fragment; and for UL44, 5′-GCCGCCGCCTACTACCC-3′ and 5′-GCTGCCGCGACTGTGATG-3′, amplifying a 661-bp fragment. The sequence of GAPDH primers used as control was as follows 5′-TGGGGAAGGTGAAGGTCGGA-3′ and 5′-GAAGGGGTCATTGATGGCAA-3′ [26]. PCR amplification of the cDNA was carried out by adding 0.5 μg of Taq DNA polymerase (Roche, Mannheim, Germany). PCR amplification of fragments was performed using 28 cycles in a DNA thermocycler using the following conditions: denaturation for 1 minute at 94°C, annealing for 2 minutes at 60°C, and extension for 2 minutes at 72°C, whereas conditions for amplification of GAPDH fragment were as follows: denaturation for 1 minute at 94°C, annealing for 1 minute at 52°C, and extension for 1.5 minutes at 72°C in a Perkin Elmer Thermocycler (Rodgau-Jügesheim, Germany). PCR products were resolved alongside DNA marker on an agarose gel, stained with ethidium bromide, and photographed.

Electron Microscopy

For ultrastructural investigations of viral infection, mice bearing KFR tumors treated with G207 as described above were sacrificed on day 2 of treatment. Electron microscopy was performed as described previously [11]. Tumor specimens were fixed in 4% formalin and 1% glutaraldehyde in monobasic phosphate buffer (pH 7.2), postfixed in 1% osmium tetroxide, dehydrated in ethanol, and imbedded in Durcupan Fluka (Sigma). Thin sections were contrasted with uranyl acetate and lead citrate, and viewed with a Jeol JEM, 2000 CX microscope (Jeol Europe, Prague, Czech Republic).

Statistics

Statistical analysis was performed using Jandel SigmaStat 2.0 (Jandel Scientific, Erkrath, Germany). Comparison between two groups was performed using Student's *t* test; three or more groups were compared by analysis of variance followed by Tukey test. *P* values less than .05 were considered significant.

Results

Susceptibility of Human Endothelial Cells to HSV-1 G207 In Vitro

The oncolytic activity of G207 was assessed *in vitro* in confluent HUVEC and HDMEC layers. The oncolytic activity of G207 in endothelial cells was compared with the effects of G207 on KFR rhabdomyosarcoma cell line and nontransformed human fibroblasts HFF. G207 exerted a direct time-dependent cytopathic effect on both endothelial cell lines. G207 infection caused cell death of 100% of HUVEC or HDMEC 3 days postinfection at an MOI of 0.1. In rhabdomyosarcoma KFR cultures, about 22% of cells survived 3 days postinfection. In contrast to this, G207 did

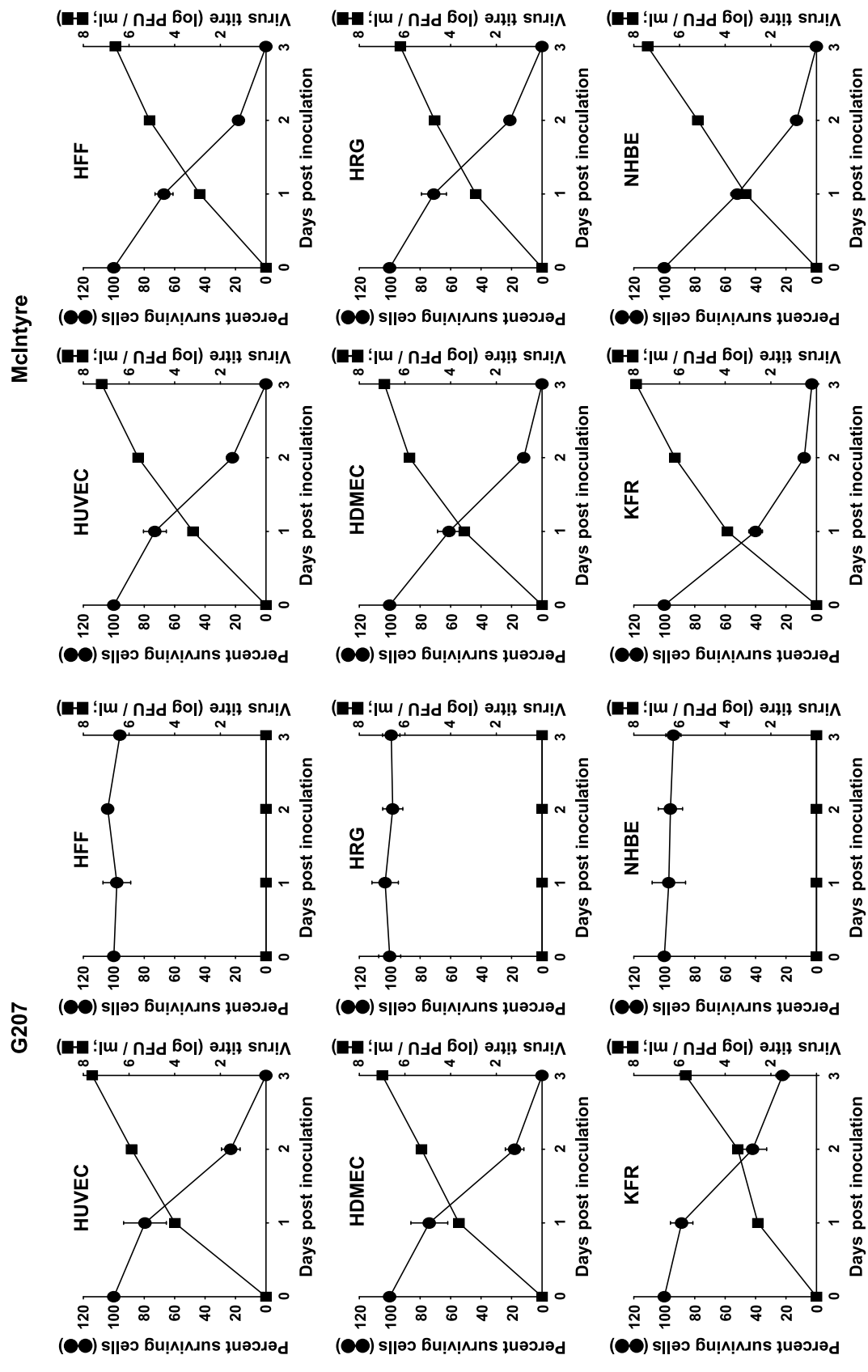

Figure 1. *Susceptibility of human endothelial cells (HUVEC and HDMEC), fibroblasts (HFF), retinal glial cells (HRG), normal human bronchial epithelial cells (NHBE), and alveolar rhabdomyosarcoma (KFR) cell cultures to G207 and HSV-1 wild-type strain McIntyre. Cells were infected with G207 or McIntyre at an MOI of 0.1. Each data point (mean of triplicate wells ± SD) is the percentage of surviving cells compared with mock-infected cells in control wells or infectious viral titers at each time point, respectively. Some error bars for data points are smaller than the symbol size.*

not influence the number of viable cells in HFF, NHBE, and HRG cultures (Figure 1). Wild-type HSV-1 strain McIntyre, an HSV-1 strain that has comparable cytopathic activity as an HSV-1 strain F (i.e., the parental strain of HSV-1 G207) [28], caused cell death to a similar extent in both normal and tumor cells (Figure 1). Furthermore, using three different HSV-1 isolates from patients yielded results comparable to HSV-1 strain McIntyre (data not shown).

Infection Efficiency and Viral Growth in Human Endothelial Cells

The efficiency of G207 infection and replication in endothelial cell cultures was demonstrated by *lacZ* expression (i.e., green-stained cells) and measurement of virus titer in infected cultures. At the time point of infection, HUVEC were all in cell cycle phase G1. Figure 2*A* shows representative pictures of HUVEC cultures 24 and 72 hours postinfection. Virus-induced cytopathogenic effects forming distinct plaques of rounded cells were detected 24 hours after infection. *LacZ* staining demonstrated 10% to 15% of *lacZ*-positive cells in the G207-infected cells after 24 hours. Strongly enhanced cytopathogenic effects were detected 3 days postinfection: cells rounded and detached from cell culture surface. More than 99% of cells stained positively for *lacZ* (Figure 2*A*). Increasing numbers of *lacZ*-positive cells correlated with increasing G207 infectious titers. Three days postinfection, HUVEC and HDMEC produced 4.1×10^7 and 9.8×10^6 PFU/ml, respectively (Figure 1). The sensitivity of HUVEC was confirmed by transmission electron microscopy demonstrating naked nucleocapsids as well as enveloped viral particles in infected cells (Figure 2*B*).

In KFR cultures, about 75% of cells were positive for *lacZ*. Viral titers also increased in a time-dependent manner. However, the viral titer, being 5.4×10^5 PFU/ml 3 days postinfection, was much lower than in endothelial cells (Figure 1). HFF, HBE, and HRG did not stain positively for *lacZ* 3 days postinfection. No infectious virus was measurable in HFF, HBE, and HRG (Figure 1). The increase of cell killing in all types of normal and tumor cells infected with HSV-1 wild-type strain McIntyre was associated with increased viral titers (Figure 1).

G207 was attenuated by inactivation of the *ICP6* gene encoding viral RR and deletion of the γ*34.5* gene that is one of the major determinants of HSV-1 neurovirulence [14]. The γ*34.5* gene deletion can be somewhat compensated by cellular Ras overexpression [27]. Therefore, inhibitors of Ras/Raf/MEK/Erk cascade and RR were used to investigate if these were able to inhibit G207 replication in HUVEC. Both manumycin A, an inhibitor of farnesyltransferases that inhibits activation of Ras [29], and the MEK inhibitor PD98059 [30] were used at concentrations that led to reduced phosphorylated Erk in HUVEC that presented a constitutively activated Ras pathway (Figure 3*A*). However, even at the highest concentrations used, both inhibitors did not influence infection efficiency as determined by the number of *lacZ*-expressing cells or cell killing (data not shown). Interestingly, HUVEC

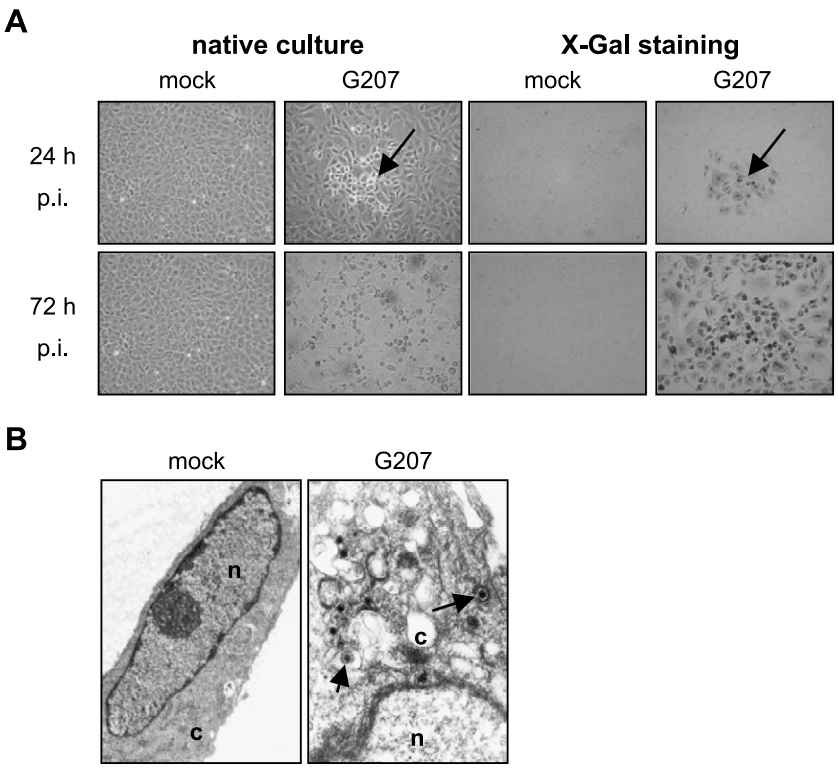

Figure 2. *Induction of cytopathogenic effect and expression of lacZ in infected HUVEC 24 and 72 hours postinfection. Arrows show G207-induced cell rounding in native cultures as well as lacZ-positive (infected) cells in cultures stained with X-gal (A). Transmission electron microscopy of cytoplasm (c) and parts of nuclei (n) of HUVEC cells showing enveloped viral particles (arrow) in the cytoplasm 48 hours postinfection (B).*

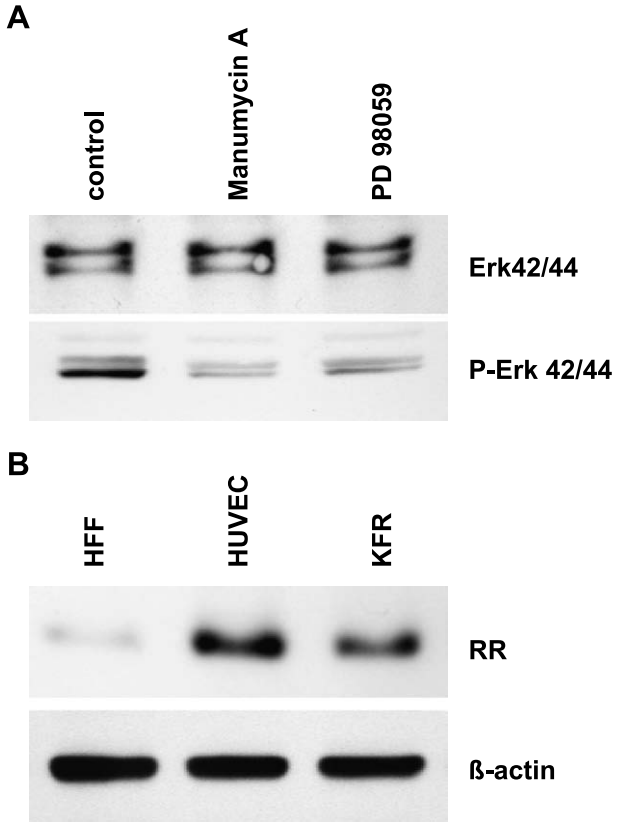

Figure 3. *Investigation of Ras pathway in HUVEC (A) and RR expression in different cell types. (B) HUVEC were exposed with the faranesyltransferase inhibitor, manumycin A, and MEK inhibitor, PD98059. Inhibitory effects of manumycin A on faranesyltransferase activity and PD98059 on MEK1/2 activity were indicated by the lack of Erk1/2 phosphorylation. (A) Protein expression profiles of cellular ribonucleotide reductase (RR, subunit M1) were observed in HFF, HUVEC, and KFR cell lines (B).*

express RR at a comparable level as KFR rhabdomyosarcoma cells, whereas HFF presented only inferior levels of RR protein (Figure 3*B*). In contrast to the mentioned Ras inhibitors, the RR inhibitor, desferrioxamine (DFO) [31], inhibited G207 replication dose-dependently between concentrations of 6.25 and 100 μM. A concentration of 100 μM completely inhibited virus infection and prevented virus-induced cell killing (Figure 4*A*). DFO treatment of mock-infected confluent HUVEC had no significant effect on cell viability. The RR inhibitor, hydroxyurea [32], inhibited G207 replication in a similar manner (not shown).

To investigate at which phase of G207 replicative cycle DFO inhibits virus infection, the effects of DFO (100 μM, added 2 hours before virus infection) on mRNA levels of different classes of viral α, β, and γ gene transcripts were observed. The transcripts of the immediate early gene α27, which is required for the subsequent production of β and γ genes [33], were present in comparable levels in both DFO-treated and untreated (control) HUVEC 4 hours postinfection. The β-gene transcripts were present at much lower levels in DFO-treated cells than in infected control cultures 24 hours postinfection. UL44 γ2 gene transcripts, which are defined as requiring the onset of viral DNA synthesis genes [33], were not detected in DFO-treated cells infected with G207 24 hours postinfection (Figure 4*B*).

Effect of G207 on Angiogenesis In Vitro

A crucial step during angiogenesis is the organization of endothelial cells into functional vessels. This process is simulated *in vitro* by the tube formation assay. Mock-infected HUVEC plated on extracellular matrix (Matrigel) formed a network of tube-like structures (Figure 5*A*). In contrast to this, tube-like structures were destroyed in cultures infected with G207 at an MOI of 0.1, 48 hours after seeding on Matrigel, but dead cells were organized in net-like structures comparable to normal tube formation indicating viral oncolysis mediated by G207 at the moment of active tube formation (Figure 5*A*). UVB-inactivated G207 did not destroy tube-like structures. Addition of acyclovir (20 μM) prevented the destruction of tube-like structures by G207. This shows that viral replication and endothelial cell lysis are essential for the destruction of tube-like structures.

Effect of G207 on Angiogenesis In Vivo

To evaluate antiangiogenic effects of G207 *in vivo*, a Matrigel plug assay was performed. Matrigel plugs supplemented with bFGF were introduced subcutaneously into mice. The plugs are supposed to contain vessels as soon as day 4 after implantation [34]. A total of 1×10^7 PFU G207 was injected into the Matrigel plug on days 1 and 3. On day 10, Matrigel plugs were removed, stained with Masson's trichrome, and investigated for endothelial cell invasion and vessel formation [35]. Plugs from control mice treated with virus buffer showed a strong invasion of endothelial cells and the formation of perfused vessels (Figure 5*B*). In contrast to this, plugs from G207-treated animals only showed weak invasion of endothelial cells. To investigate, if virus replication was necessary for antiangiogenic effects, UVB-inactivated G207 was injected into the plugs on days 1 and 3. Injection of inactive virus resulted in endothelial cell invasion and vessel formation comparable to control.

Replication of G207 in Tumor and Endothelial Cells

Previously, we demonstrated that intratumoral treatment of KFR tumors in nude mice inhibited tumor growth due to virus replication and spreading in tumor cells [11]. Consistent with these results, Figure 6*A* shows that intratumoral treatment with G207 inhibited KFR tumor growth in all animals and induced complete tumor disappearance in four of seven. Eight days after virus injection, histochemical examination of control tumors showed a morphology that is typical for ARMS, with many perfused microcapillaries (in the hotspot sites of tumors, 18 ± 4.2 vessels were detected), whereas G207-treated tumors were composed of necrotic cells without any microcapillaries (Figure 6*B*). To show whether G207 may infect endothelial cells, G207-treated tumors were examined by electron microscopy. Ultrastructural investigations showed viral particles in tumor and endothelial cells of treated xenografts (Figure 6*C*), but not in adjacent normal tissues 24 hours after G207 injection (not shown).

Discussion

In the present study, we showed for the first time that an oncolytic virus inhibits angiogenesis. In addition, this is the first report that demonstrates the productive infection of endothelial cells from different origins by the oncolytic virus, HSV-1 G207. UVB irradiation of viral particles or treatment with antiviral agent acyclovir prevented the inhibition of *in vitro* tube formation and vessel formation in the *in vivo* Matrigel assay induced by G207 infection. These results show that viral replication is essential for antiangiogenic effects of G207.

The finding that G207 replicates in confluent endothelial cell cultures is somewhat surprising because the multimutated oncolytic virus was designed to selectively replicate in dividing transformed cells. In fact, human normal (nontransformed) cells including dermal fibroblasts, bronchial epithelial cells, and HRG did not promote replication of G207 as demonstrated by the failure to produce infectious virus and to

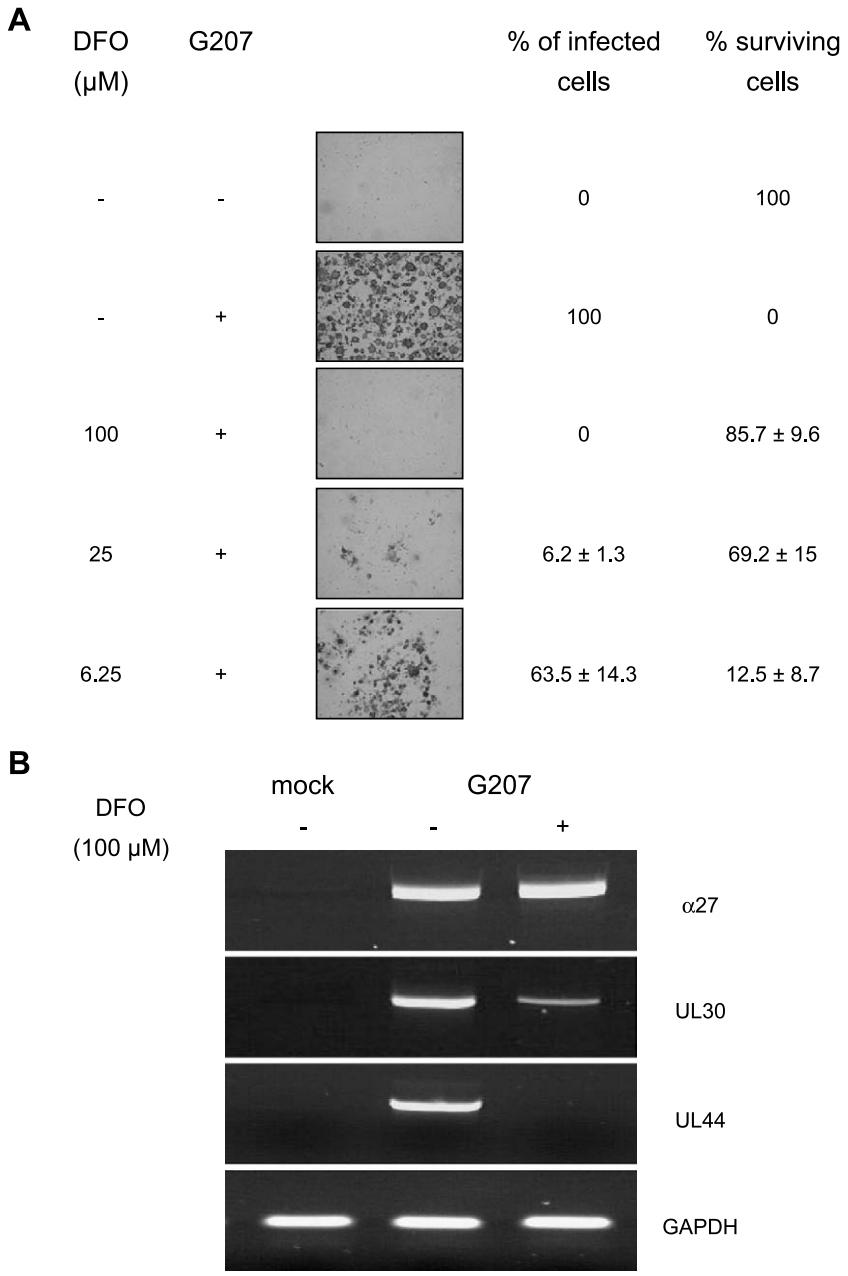

Figure 4. *Infection efficiency and cell killing of HUVEC treated with DFO at concentrations ranging from 6.25 to 100 μM. DFO was added to cell cultures 2 hours before virus infection. Infection efficiency was examined 72 hours postinfection by calculation of the percentage of lacZ-positive cells, and viable cells were counted using the trypan blue exclusion method. Each data point (mean of triplicate wells ± SD) is the percentage of cells expressing β-galactosidase or surviving cells compared with mock-infected cells in control wells, respectively (A). Effects of DFO (100 μM, added 2 hours before virus infection) on G207 replicative cycle in HUVEC. Cells were collected and cytoplasmatic RNA was extracted at 4 and 24 hours after virus infection. mRNA levels of HSV-1–specific α-gene (α27) were detected 4 hours after virus infection, whereas β-gene (UL30) and γ-gene (UL44) were measured 24 hours after virus infection. RT-PCR products were separated on a 1.5% agarose gel and visualized with ethidium bromide under ultraviolet light (B).*

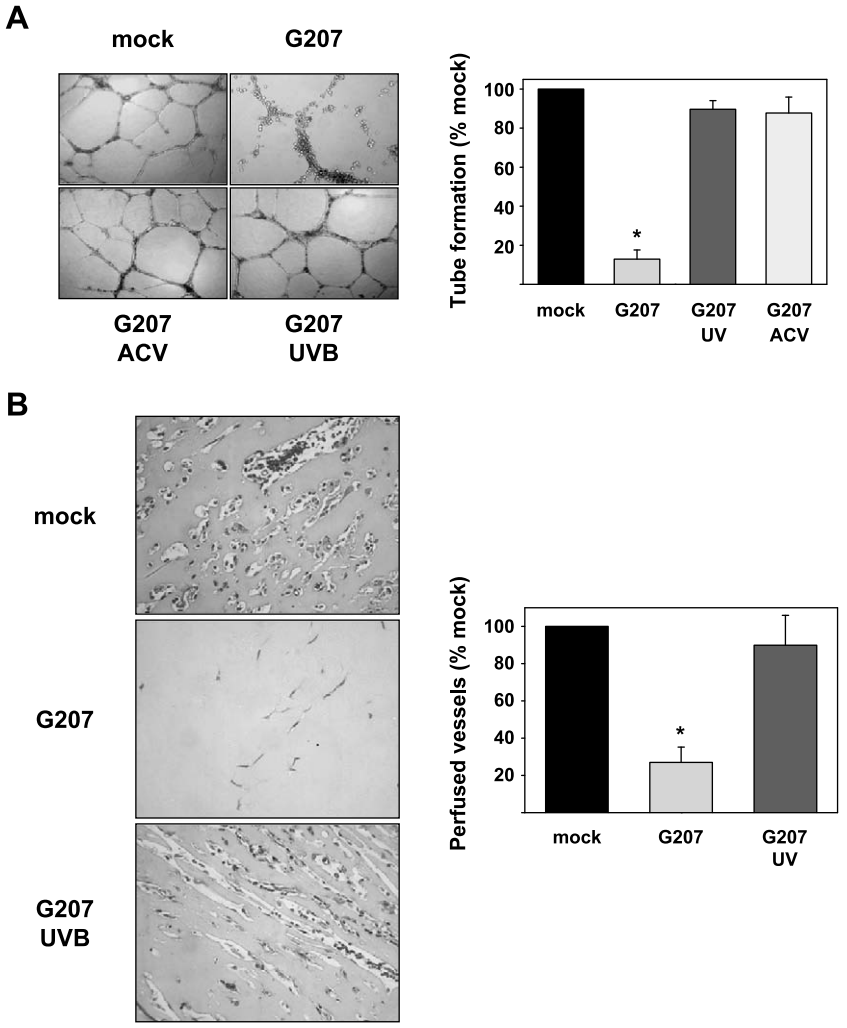

Figure 5. *Effects on angiogenesis in vitro (A) and in vivo (B). Infection of HUVEC at an MOI of 0.1 significantly suppressed in vitro tube-like formation (P < .001), whereas the effects were not observed after treatment with acyclovir (20 μM) or infection with G207 inactivated by UVB (A). G207 significantly prevented the formation of perfused vessels in the in vivo Matrigel plug assay (P < .001). In contrast, similar numbers of perfused vessels were observed in Matrigel plugs after mock infection or infection with UVB-irradiated G207 (B).*

destroy cells in infected cultures. However, these normal cell types were highly sensitive to replicative and cytotoxic effects of wild-type HSV-1. Therefore, unlike other normal cell types, endothelial cells seem to be unique in their susceptibility to G207.

G207 is derived from HSV-1 mutant *R3616*, which contains deletions in both loci of the *γ34.5* gene that is required for replication in the central nervous system [12,13]. HSV-1 infection leads to the activation of double-stranded RNA-activated protein kinase (PKR). PKR causes phosphorylation and therefore inactivation of the α-subunit of eukaryotic translation initiation factor 2 (eIF2α), leading to inhibition of cellular translation [36]. The gene product of γ134.5 (called ICP34.5) presumably forms a complex with protein phosphatase 1 (PP1), leading to dephosphorylation/activation of eIF2α and restoring cellular translation in HSV-1–infected cells [37]. Thus, the absence of ICP34.5 results in the inhibition of translation of the viral transcripts in normal (nontransformed) cells. Ras-transfected cells are able to compensate for the lack of ICP34.5 and are permissive to infection, with HSV-1 mutants lacking the *γ34.5* gene [27]. Because Ras is constitutively activated in a high number of different tumors [38], destruction of the *γ134.5* gene limits specific virus replication to Ras-overexpressing tumor cells. Ras leads to inhibition of PKR phosphorylation/activation and, in turn, to phosphorylation/inactivation of eIF2α. Treatment of Ras-overexpressing cells with a farnesyl transferase inhibitor that inhibits the activation of Ras or PD98059, an inhibitor of the downstream signal protein of Ras MEK, inhibited HSV-1 *R3616* replication in Ras-overexpressing cells to some extent [27]. This shows that the inhibition of PKR phosphorylation by Ras overexpression is, at least in part, mediated by the Ras/Raf/MEK cascade. To evaluate the importance of the Ras/Raf/MEK cascade for replication of G207 in endothelial cells, endothelial cells were infected with G207 in the presence of the farnesyltransferase inhibitor, manumycin A, or the MEK inhibitor, PD98059. Neither manumycin A nor PD98059 exhibited significant effects on G207 replication or cell killing in infected endothelial cultures, despite the fact that both inhibitors reduced significantly the

level of phosphorylated Erk in treated HUVEC. Thus, we suggest that the Ras pathway does not play an essential role for replication of G207 in endothelial cells.

To further ensure that G207 is unable to replicate in normal quiescent cells, the viral *ICP6* gene, encoding the large subunit of viral RR (the enzyme that reduces ribonucleotides to deoxyribonucleotides necessary for DNA synthesis), was inactivated in G207 [14]. This genetic modification renders the replication of G207 dependent on the presence of cellular RR. Dividing normal cells that express high levels of cellular RR activity can be destroyed by HSV-1 strains lacking RR. Oncolytic HSV-1 strain hrR3 with inactivated RR gene was shown to infect and selectively kill actively proliferating rat retinal pigment epithelial cells while sparing normal nonreplicating cells [39]. Moreover, upregulation of RR by ionizing radiation potentiated G207 replication. Chemical RR inhibition using hydroxyurea abrogated enhanced replication again [40]. In concordance with these findings, nonreplicating confluent HFF that are permissive to infection by wild-type HSV-1 were nonpermissive to G207. Confluent endothelial cells, however, were highly permissive to G207 infection. HUVEC and KFR rhabdomyosarcoma cells express high levels of RR in comparison to HFF cells. Addition of two RR inhibitors, namely DFO and hydroxyurea, prior to virus infection resulted in a dose-dependent suppression of G207 replication in HUVEC. Investigation of mRNA levels of viral genes expressed at different phases of viral replication cycle revealed that RR inhibitors inhibited G207 replication but did not influence viral adsorption and penetration. This suggests that cellular RR activity, in accordance with other studies, is most probably responsible for G207 replication in confluent endothelial cells [4,40–42].

In addition to the effects on endothelial cells, our present study confirmed previous results demonstrating that G207 infects and destroys KFR cells *in vitro* and inhibits growth of KFR xenografts in mice [11]. The sensitivity of KFR cells to G207 infection complicates the rating of the impact of G207-caused angiogenesis inhibition on tumor development in this model. Nevertheless, the complete absence of tumor vessels in G207-treated tumors and the detection of virus particles in tumor endothelial cells clearly demonstrate the inhibition of tumor angiogenesis by G207. Further investigations will have to study the influence of G207 on growth and vessel formation of tumors, which are nonpermissive to G207. It is also important to compare the sensitivity of

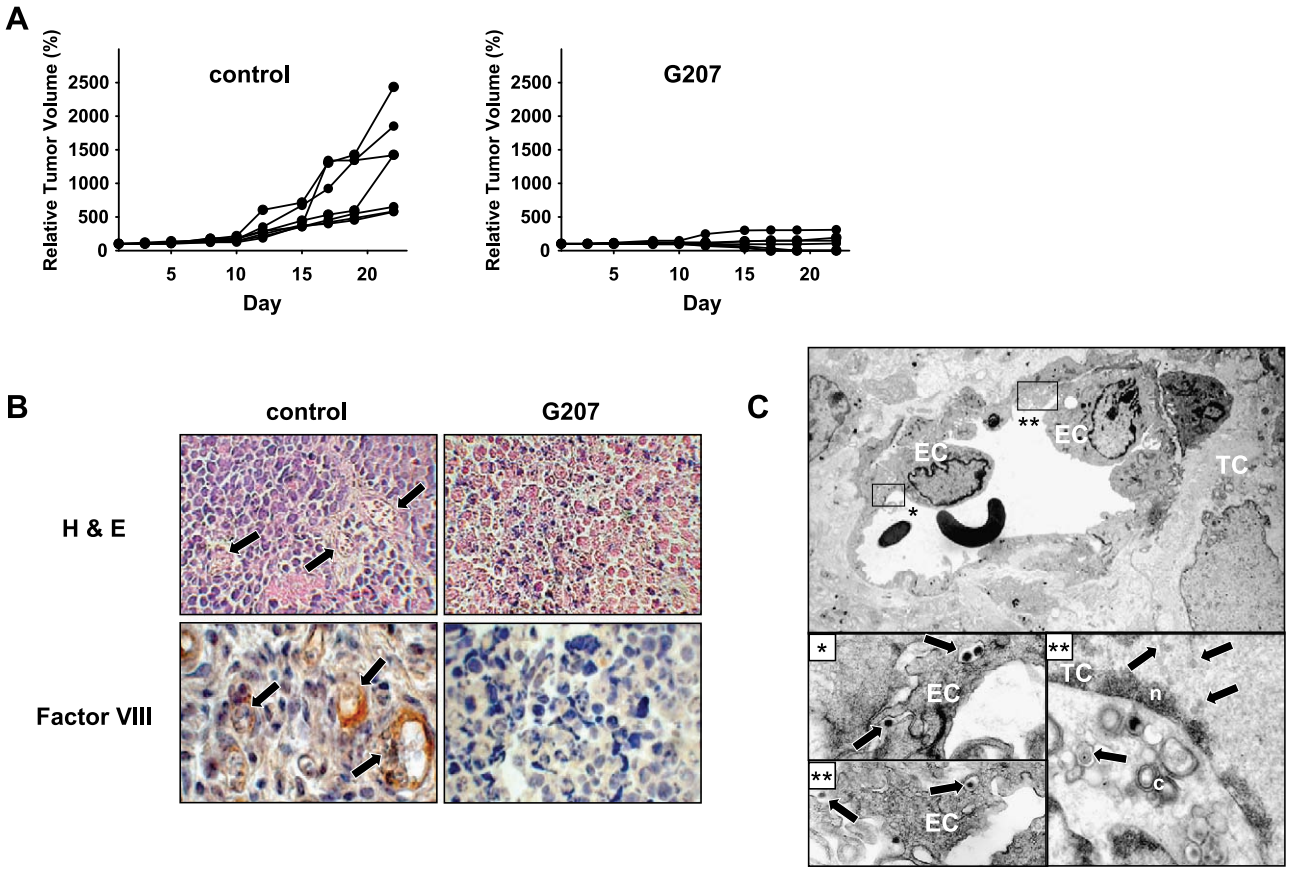

Figure 6. *Xenografts of subcutaneous KFR tumors treated with intrathecal. G207. Growth curves of control (saline-treated) and G207-treated established KFR tumors after the start of treatment (A). Examination of thin sections stained with H&E show tumor vessels filled with erythrocytes (arrows) and immunoperoxidase staining with anti–mouse Factor VIII antiserum depicts endothelial cells of tumor microvessels (arrows). Endothelial cells were not detected in tumors 8 days after G207 injection (B). Detection of G207 in endothelial cells of KFR xenografts 24 hours after G207 treatment. Enveloped viral particles are frequently enclosed in vacuoles in the cytoplasm of endothelial cells, which are shown in greater magnification in insets. Furthermore, enveloped viral particles in the cytoplasm and nucleocapsids in nucleus are shown in a tumor cell (C). EC = endothelial cell; TC = tumor cell; n = nucleus; c = cytoplasm.*

tumor-associated endothelial cells to G207 with that of the normal endothelium of different organs. Although this item was not addressed in the present study, ultrastructural investigations failed to demonstrated G207 particles in adjacent normal tissues. Moreover, previous animal studies showed that G207 does not disseminate and replicate in normal cells of different organs [11,43,44].

Angiogenesis is considered to play a central role in tumor growth and metastasis formation. Numerous antiangiogenic agents are under clinical evaluation in phase II and phase III trials [22,45]. Oncolytic viruses such as G207 represent an interesting new therapeutical approach to suppress tumor angiogenesis because their mode of action differs from that of other antiangiogenic drugs. New investigations indicated that clinical use of angiogenesis inhibitors is more complicated as initially expected. Therefore, establishment of proper treatment schedules and a combination of different antiangiogenic agents is regarded as necessary to achieve efficient angiogenesis inhibition and, consequently, anticancer activity in patients [22]. G207 appears to be a very well-suited additional tool for angiogenesis inhibition, alone or in combination with other antiangiogenic agents or therapy strategies. We have already demonstrated that combination with vincristine drastically enhanced the anticancer activity of G207 in a xenotransplanted rhabdomyosarcoma model [11]. Similarly, increased cell killing of a human non small cell lung cancer cell line treated with the combination of oncolytic HSV-1 1716 and mitomycin C has been demonstrated [46]. Because nontoxic frequent low dosing of cytotoxic agents was shown to suppress tumor growth by inhibition of angiogenesis in several experimental models, the combination of G207 with cytotoxic drugs should be investigated as a new antiangiogenic strategy [21,22].

In conclusion, this report shows that infection with oncolytic HSV-1 G207 inhibits angiogenesis, including tumor-induced vessel formation. Viral replication in endothelial cells is necessary for the inhibition of angiogenesis. The antiangiogenic mechanism of G207 differs from that of all known antiangiogenic agents under evaluation. Our study provides new insights into the antitumoral function of oncolytic G207 and opens a new field of therapeutic concepts that should be combined with G207 against cancer in humans.

Acknowledgements

We thank Samuel D. Rabkin for helpful discussion and critical reading of this manuscript. The authors thank Lena Stegmann and Gesa Meincke for their skillful technical assistance.

References

[1] Kirn D, Martuza RL, and Zwiebel J (2001). Replication-selective virotherapy for cancer: biological principles, risk management and future directions. *Nat Med* **7,** 781–787.

[2] Toda M, Rabkin SD, and Martuza RL (1998). Treatment of human breast cancer in a brain metastatic model by G207, a replication-competent multimutated herpes simplex virus 1. *Hum Gene Ther* **9,** 2177–2185.

[3] Walker JR, McGeagh KG, Sundaresan P, Jorgensen TJ, Rabkin SD, and Martuza RL (1999). Local and systemic therapy of human prostate adenocarcinoma with the conditionally replicating herpes simplex virus vector G207. *Hum Gene Ther* **10,** 2237–2243.

[4] Kooby DA, Carew JF, Halterman MW, Mack JE, Bertino JR, Blumgart LH, Federoff HJ, and Fong Y (1999). Oncolytic viral therapy for human colorectal cancer and liver metastases using a multi-mutated herpes simplex virus type-1 (G207). *FASEB J* **13,** 1325–1334.

[5] Coukos G, Makrigiannakis A, Montas S, Kaiser LR, Toyozumi T, Benjamin I, Albelda SM, Rubin SC, and Molnar-Kimber KL (2000). Multi-attenuated herpes simplex virus-1 mutant G207 exerts cytotoxicity against epithelial ovarian cancer but not normal mesothelium and is suitable for intraperitoneal oncolytic therapy. *Cancer Gene Ther* **7,** 275–283.

[6] Chahlavi A, Todo T, Martuza RL, and Rabkin SD (1999). Replication-competent herpes simplex virus vector G207 and cisplatin combination therapy for head and neck squamous cell carcinoma. *Neoplasia* **1,** 162–169.

[7] Todo T, Martuza RL, Rabkin SD, and Johnson PA (2001). Oncolytic herpes simplex virus vector with enhanced MHC class I presentation and tumor cell killing. *Proc Natl Acad Sci USA* **98,** 6396–6401.

[8] Todo T, Rabkin SD, Chahlavi A, and Martuza RL (1999). Corticosteroid administration does not affect viral oncolytic activity, but inhibits antitumor immunity in replication-competent herpes simplex virus tumor therapy. *Hum Gene Ther* **10,** 2869–2878.

[9] Todo T, Rabkin SD, Sundaresan P, Wu A, Meehan KR, Herscowitz HB, and Martuza RL (1999). Systemic antitumor immunity in experimental brain tumor therapy using a multimutated, replication-competent herpes simplex virus. *Hum Gene Ther* **10,** 2741–2755.

[10] Bharatan NS, Currier MA, and Cripe TP (2002). Differential susceptibility of pediatric sarcoma cells to oncolysis by conditionally replication-competent herpes simplex viruses. *J Pediatr Hematol Oncol* **24,** 447–453.

[11] Cinatl J Jr, Cinatl J, Michaelis M, Kabickova H, Kotchetkov R, Vogel J-U, Doerr HW, Klingebiel T, and Hernáiz Driever P (2003). Potent oncolytic activity of multimutated herpes simplex virus G207 in combination with vincristine against human rhabdomyosarcoma. *Cancer Res* **63,** 1508–1514.

[12] Roizman B and Markovitz N (1997). Herpes simplex virus virulence: the functions of the gamma (1)34.5 gene. *J Neurovirol* **3,** S1–S2.

[13] Chou J, Kern ER, Whitley RJ, and Roizman B (1990). Mapping of herpes simplex virus-1 neurovirulence to gamma 134.5, a gene nonessential for growth in culture. *Science* **250,** 1262–1266.

[14] Mineta T, Rabkin SD, and Martuza RL (1994). Treatment of malignant gliomas using ganciclovir-hypersensitive, ribonucleotide reductase–deficient herpes simplex viral mutant. *Cancer Res* **54,** 3963–3966.

[15] Goldstein DJ and Weller SK (1988). Herpes simplex virus type 1–induced ribonucleotide reductase activity is dispensable for virus growth and DNA synthesis: isolation and characterization of an *ICP6 lacZ* insertion mutant. *J Virol* **62,** 196–205.

[16] Carroll NM, Chiocca EA, Takahashi K, and Tanabe KK (1996). Enhancement of gene therapy specificity for diffuse colon carcinoma liver metastases with recombinant herpes simplex virus. *Ann Surg* **224,** 323–329.

[17] Mineta T, Rabkin SD, Yazaki T, Hunter WD, and Martuza RL (1995). Attenuated multi-mutated herpes simplex virus-1 for the treatment of malignant gliomas. *Nat Med* **1,** 938–943.

[18] Mohr I and Gluzman Y (1996). A herpesvirus genetic element which affects translation in the absence of the viral GADD34 function. *EMBO J* **15,** 4759–4766.

[19] Folkman J (1971). Tumor angiogenesis: therapeutic implications. *N Engl J Med* **285,** 1182–1186.

[20] Folkman J (1990). What is the evidence that tumors are angiogenesis dependent? *J Natl Cancer Inst* **82,** 4–6.

[21] Miller KD, Sweeney CJ, and Sledge GW Jr (2001). Redefining the target: chemotherapeutics as antiangiogenics. *J Clin Oncol* **19,** 1195–1206.

[22] Kerbel R and Folkman J (2002). Clinical translation of angiogenesis inhibitors. *Nat Rev Cancer* **2,** 727–739.

[23] Michaelis M, Michaelis UR, Fleming I, Suhan T, Cinatl J, Blaheta RA, Hoffmann K, Kotchetkov R, Busse R, Nau H, and Cinatl J Jr (2004). Valproic acid inhibits angiogenesis *in vitro* and *in vivo*. *Mol Pharmacol* **65,** 520–527.

[24] Cinatl J Jr, Bittoova M, Margraf S, Vogel J-U, Cinatl J, Preiser W, and Doerr HW (2000). Cytomegalovirus infection decreases expression of thrombospondin-1 and -2 in cultured human retinal glial cells: effects of antiviral agents. *J Infect Dis* **182,** 643–651.

[25] Cinatl J Jr, Cinatl J, Hernáiz Driever P, Rabenau H, Hovak M, Benda R, Gümbel HO, Kornhuber B, and Doerr HW (1994). Induction of

myogenic differentiation in a human rhabdomyosarcoma cell line by phenylacetate. *Cancer Lett* **78,** 41–48.

[26] Cinatl J Jr, Margraf S, Vogel J-U, Scholz M, Cinatl J, and Doerr HW (2001). Human cytomegalovirus circumvents NF-kappa B dependence in retinal pigment epithelial cells. *J Immunol* **167,** 1900–1908.

[27] Farassati F, Yang AD, and Lee PW (2001). Oncogenes in Ras signalling pathway dictate host-cell permissiveness to herpes simplex virus 1. *Nat Cell Biol* **3,** 745–750.

[28] LaVail JH, Topp KS, Giblin PA, and Garner JA (1997). Factors that contribute to the transneuronal spread of herpes simplex virus. *J Neurosci Res* **49,** 485–496.

[29] Hara M, Akasaka K, Akinaga S, Okabe M, Nakano H, Gomez R, Wood D, Uh M, and Tamanoi F (1993). Identification of Ras farnesyltransferase inhibitors by microbial screening. *Proc Natl Acad Sci USA* **90,** 2281–2285.

[30] Dudley DT, Pang L, Decker SJ, Bridges AJ, and Saltiel AR (1995). A synthetic inhibitor of the mitogen-activated protein kinase cascade. *Proc Natl Acad Sci USA* **92,** 7686–7689.

[31] Hoffbrand AV, Ganeshaguru K, Hooton JW, and Tattersall MH (1976). Effect of iron deficiency and desferrioxamine on DNA synthesis in human cells. *Br J Haematol* **33,** 517–526.

[32] Elford HL (1968). Effect of hydroxyurea on ribonucleotide reductase. *Biochem Biophys Res Commun* **33,** 129–135.

[33] Roizman B and Knipe DM (2001). Herpes simplex viruses and their replication. In *Field's Virology* (Vol. 2, 4th ed). Knipe DM and Howley PM (Eds). Lippincott, Philadelphia, PA, pp. 2399–2459.

[34] Akhtar N, Dickerson EB, and Auerbach R (2002). The sponge/Matrigel angiogenesis assay. *Angiogenesis* **5,** 75–80.

[35] Auerbach R, Lewis R, Shinners B, Kubai L, and Akhtar N (2003). Angiogenesis assays: a critical overview. *Clin Chem* **49,** 32–40.

[36] Andreansky SS, He B, Gillespie GY, Soroceanu L, Markert J, Chou J, Roizman B, and Whitley RJ (1996). The application of genetically engineered herpes simplex viruses to the treatment of experimental brain tumors. *Proc Natl Acad Sci USA* **93,** 11313–11318.

[37] He B, Gross M, and Roizman B (1997). The gamma(1)34.5 protein of herpes simplex virus 1 complexes with protein phosphatase 1 alpha to dephosphorylate the alpha subunit of the eukaryotic translation initiation factor 2 and preclude the shutoff of protein synthesis by double-stranded RNA-activated protein kinase. *Proc Natl Acad Sci USA* **94,** 843–848.

[38] Bos JL (1989). *ras* oncogenes in human cancer: a review. *Cancer Res* **49,** 4682–4689.

[39] Wong CA, Jia W, and Matsubara JA (1999). Experimental gene therapy for an *in vitro* model of proliferative vitreoretinopathy. *Can J Ophthalmol* **34,** 379–384.

[40] Stanziale SF, Petrowsky H, Joe JK, Roberts GD, Zager JS, Gusani NJ, Ben Porat L, Gonen M, and Fong Y (2002). Ionizing radiation potentiates the antitumor efficacy of oncolytic herpes simplex virus G207 by up-regulating ribonucleotide reductase. *Surgery* **132,** 353–359.

[41] Petrowsky H, Roberts GD, Kooby DA, Burt BM, Bennett JJ, Delman KA, Stanziale SF, Delohery TM, Tong WP, Federoff HJ, and Fong Y (2001). Functional interaction between fluorodeoxyuridine-induced cellular alterations and replication of a ribonucleotide reductase–negative herpes simplex virus. *J Virol* **75,** 7050–7058.

[42] Reinblatt M, Pin RH, Federoff H, and Fong Y (2004). Utilizing tumor hypoxia to enhance oncolytic viral therapy in colorectal metastases. *Ann Surg* **239,** 892–902.

[43] Hunter WD, Martuza RL, Feigenbaum F, Todo T, Mineta T, Yazaki T, Toda M, Newsome JT, Platenberg RC, Manz HJ, and Rabkin SD (1999). Attenuated, replication-competent herpes simplex virus type 1 mutant G207: safety evaluation of intracerebral injection in nonhuman primates. *J Virol* **73,** 6319–6326.

[44] Sundaresan P, Hunter WD, Martuza RL, and Rabkin SD (2000). Attenuated, replication-competent herpes simplex virus type 1 mutant G207: safety evaluation in mice. *J Virol* **74,** 3832–3841.

[45] Verheul HM, Voest EE, and Schlingemann RO (2004). Are tumours angiogenesis-dependent? *J Pathol* **202,** 5–13.

[46] Toyoizumi T, Mick R, Abbas AE, Kang EH, Kaiser LR, and Molnar-Kimber KL (1999). Combined therapy with chemotherapeutic agents and herpes simplex virus type 1 ICP34.5 mutant (HSV-1716) in human non-small cell lung cancer. *Hum Gene Ther* **10,** 3013–3029.